Sunflower ashes and nanoparticles embedded in silane matrix as bioactive filler material

Romina A. Arreche[a,*], Natalia Bellotti[b], Patricia G. Vázquez[a]

[a]CINDECA - Centro de Investigación y Desarrollo en Ciencias Aplicadas, ¨Dr. Jorge J. Ronco¨, CCT La Plata, CONICET - Departamento de Química, Facultad de Ciencias Exactas, UNLP, 47 Nº 257 (1900), La Plata, Buenos Aires, Argentina.
[b]CIDEPINT - Centro de Investigación y Desarrollo en Tecnología de Pinturas (CIC - CONICET), Calle 52 e/121 y 122 (1900), La Plata, Buenos Aires, Argentina.
*E-mail address: arrecheromina@quimica.unlp.edu.ar

Abstract

Microbial contamination of indoor environmental surfaces is a common source for infections therefore, bio-deterioration in buildings indoor materials is really important to avoid, due to the negative impact on human health. Consequently, functionalized and sustainable materials are being intensively studied to control the microbial colonization. Firstly, it was possible to obtain silica samples by the sol-gel method with the addition of sunflower residues in the form of ashes together with silver or copper salt to produce antimicrobials solids. Secondly, the synthesized solids were characterized by different techniques. TEM analyses confirmed the successful inclusion of silver and copper nanoparticles into the silica framework mainly spherical in shape, and small size. The antimicrobial activity of the solids was assessed against fungal strains obtained from indoor bio-deteriorated building surfaces, *Chaetomium globosum* (KU936228) and *Alternaria alternata* (KU936229). The addition of ashes into the samples improved the antifungal activity of the solids. Both silver and copper as antimicrobial agents reduce the potential for cross-contamination to occur, as it is effective against a wide range of microorganisms.

Keywords: sol-gel, bioactive silica, sunflower ashes, Ag nanoparticles, Cu nanoparticles; antimicrobial materials.

1. **Introduction**

In the contemporary world two major point are relevant enough, the sustainability and the health care. On the one hand, the sustainability is a topic that concerns both the agendas of politicians and the strategies of companies and their implementation are increasingly valuated in different process. The term sustainability itself originates in the French verb *soutenir,* "to hold up or support" [1]. The Brundtland Commission also provided the most commonly accepted definition of sustainability as "development that meets the needs of the present without compromising the ability of future generations to meet their own needs" [2]. Taking into account the maintenance of the holistic, adaptive and flexible nature that sustainability gives, it can be said that sustainability is framed as the balanced and systemic integration of economic, social and environmental performance within and between generations [3]. Sustainability opens up multiple questions about, for example, what should be developed and what should be sustained, for how long and for whose benefit [4]. The concept of the Circular Economy has been gaining momentum since the late 1970s. Based on different contributions, Geissdoerfer et al. [5] defined the Circular Economy as ¨a regenerative system in which resource input and waste, emission, and energy leakage are minimized by slowing, closing, and narrowing material and energy loops. This can be achieved through long-lasting design, maintenance, repair, reuse, remanufacturing, refurbishing, and recycling¨.

In relation to health care, there is a basic need in medical science to assess the medical state of an individual. Hippocratic textbooks advised doctors to examine their patient for "signs" to assist clinical decision-making [6]. Health forecasting is a new area of forecasting, and a valuable tool for predicting future health events or situations, such as demands for health services and medical care and needs. Preventive medicine and healthcare facilitate intervention strategies, previously informing health service providers so that they can take appropriate mitigation measures to minimize risks and manage demand [7]. However, the interaction between pathogenic bacteria, opportunistic strains, and harmful and beneficial microbes in hospitals and in contaminated spaces in general, it is not understood and more research is still needed.

Some evidence has recognized microbial contamination of indoor environmental surfaces as frequent source for infections [8]. Inanimate surfaces have often been described as the source for outbreaks of nosocomial infections, the most common nosocomial pathogens may well survive or persist on surfaces for months and can thereby be a continuous source of transmission if no regular preventive surface disinfection is performed [9]. Therefore, new materials need to be developed to control or prevent microbial contamination [10]. The association of an antimicrobial agent in an organic or inorganic matrix to be used in paints, coatings or another material as functionalized filler is an interesting way to achieve the mentioned problem [11]. Polymeric matrix functionalized with an antimicrobial agent seeks to improve its performance as part of bioactive material due to chemically stabilization that maintains its effectiveness over time [12-14]. Sol-gel method is a simple tool that allows obtaining solids with different porosity at low temperatures, as well as the immobilization of metals and other chemical species by electrostatic interaction, adsorption and covalent bond [15; 16]. In addition, the inclusion of bioactive chemical species into the silica matrix could be achieved by impregnation, dissolution or suspension into the gel [17; 18].

Due to the increasing resistance against the antibiotics and also the knowledge about the antimicrobial properties of metals with superior characteristics such as safety, durability and heat resistance in comparison with the conventional organics biocides, silver and copper salts are being intensively studied for various applications [19-21]. In this sense, Ag and/or Cu have been applied in several fields, such as medicine, food industry, paint/coating technology and water treatment, among others [22-31]. Particularly, there are in the literature some researches about immobilization of Ag in materials obtained by the sol-gel method [32; 33].

In this work, silver salt ($AgNO_3$) or copper salt ($CuNO_3$) were used during sol-gel process with the goal to obtain antimicrobial functionalized materials. We report a simple and green way to synthesize bioactive silica with the incorporation of sunflower ashes. The ashes were obtained from the edible oil industrial waste [34] and was added as filler material into the silica solids. The sunflower is widely cultivated worldwide and Argentina is one of the most important producer countries, producing about half of world production of sunflower seed [35]. The sunflower husk represents a percentage by weight of 45%–60% of the seed

and is widely used for the production of feed, biomass [36], solid biofuel [37; 38], but their use as filler in materials is very scarce.

The solids synthesized was characterized using transmission electron microscopy (TEM), scanning electron microscopy (SEM), Fourier transform infrared spectroscopy (FTIR), adsorption-desorption of N_2 (S_{BET}), potentiometric titration with *n*-butylamine and, the % of moisture and zeta potential were measured.

The antimicrobial activity of the solids obtained was assessed against fungal strains: *Chaetomium globosum* (KU936228) and *Alternaria alternata* (KU936229), previously obtained from indoor bio-deteriorated building surfaces [21]. These fungi were selected for their ability to grow easily on materials and their negative impact on human health due to their ability to produce a variety of compounds including mycotoxins, which are toxic to mammals [39]. Infections and health problems resulted from poor indoor environmental quality has increased the interest over time due to increasing evidence indicating the importance of controlling the development of biofilms in such places [21; 39].

The focus of this study was to prepare new materials from non-toxic chemicals, by using the 'Green Chemistry' tools, providing solutions to technological and ecological challenges in different areas. In this work, one of the principles is to design a synthesis route for the production of materials for health and the environment care.

2. Materials and methods

2.1. Synthesis of silica

The siliceous solids were prepared by the sol-gel method under a N_2 atmosphere. Tetraethyl orthosilicate (TEOS) ($Si(OCH_3)_4$ - 98%) was used as precursor, nitric acid (HNO_3 - 65 %) as catalyst of the sol-gel reaction, whereas absolute ethanol (CH_2CH_3OH - 99.9%) and distilled water (DW) were employed as solvents. The molar ratios of the reagents used in the synthesis were 1.00:1.17:5.00:3.73 for precursor/catalyst/solvent/water, respectively. First, the catalyst was mixed with half amount of ethanol, then TEOS was added to the mixture and after that, silver nitrate ($AgNO_3$ - 99.99%) or cupric nitrate ($Cu(NO_3)_2$ - pure) was incorporated with another half of ethanol and water. Finally, different amounts of ashes from sunflower husk were incorporated to the synthesis (Figure 1). The homogeneous solution obtained was stirred vigorously for 12 h and kept at room temperature for 7 days

for gelation and drying. The nomenclature used for the solids were: S0, for unmodified silica, SA, for the silica modified with different concentrations of ashes (1% or 10% w/w), and SAAg or SACu for the silica modified with ashes together with silver salt or cupric salt (1% or 2% w/w), respectively.

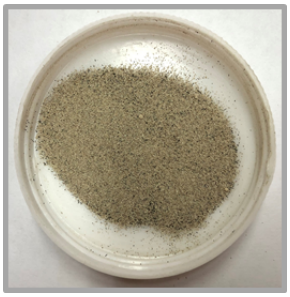

Figure 1 Ashes from Sunflower-seed husk

The concentration of ashes used in the synthesis was selected according to their volume, being 1% and 10% w/w adequate limit weigh. In relation to silver and copper concentration, the amounts used were selected by using previous works data [40].

2.2. Characterization of the solids

The textural properties of the solids, such as the specific surface area (S_{BET}), the pore volume and pore size, were determined by adsorption/desorption in Micromeritics Accusorb 2100 equipment (USA), using N_2 as absorbable gas. Before the measurement, each sample was degassed at 100 °C for 12 h.

The measurement of the % moisture was carried out employing a BOECO MBO-35 analytical balance (Germany), 0.500 mg of the solid was weighted and, after a heating treatment of the sample at 110 °C for 90 min, the weight loss (%) was recorded as the moisture content of samples. Each measurement was carried out by triplicate.

Zeta potential of silica particles was determined using Zetasizer Nano-ZS90 (Malvern Instruments). The analysis was carried out at a scattering angle of 90°, at 25 °C, using samples diluted with Milli-Q distilled water. Five measures were performed for each synthesized sample.

The evaluation of the acidic properties of solids was carried out by potentiometric titration with *n*-butylamine, in a Metrohm 794 Basic Titrino titrator (Switzerland), with a double-

junction electrode. 0.025 mL/min of an *n*-butylamine solution in acetonitrile (0.025 N) was added to 0.025 g of sample, previously suspended in 45 mL of acetonitrile, keeping the stirring time, before to add the first drop, constant (540 s) and a waiting time of the drop of 60 s, while stirring constantly.

FT-IR (Fourier transform infrared spectroscopy) spectra were obtained using Bruker IFS 66 equipment (Germany) and pellets of the sample in KBr, at room temperature, measured in a range between 400 and 4000 cm^{-1}.

Scanning electron microscopy (SEM) was carried out to obtain different micrographs of the solids, in JEOL equipment, JSM-6390LV (Japan), using a voltage of 20 kV. Samples were supported on graphite and metallized with a sputtered gold film.

TEM (Transmission electron microscopy) measurements were performed on a JEOL (model JEM 2011) instrument, operated at an accelerating voltage of 120 kV. Samples were prepared by their suspension in milli-Q water and placing 5 μL over carbon-coated copper grids, allowing the samples to dry in a desiccator for 16 h at room temperature.

2.3. Antifungal activity

The antifungal activity of selected samples was assessed against *Chaetomium globosum* (KU936228) and *Alternaria alternata* (KU936229) isolated in a previous work [21]. The dilution method employed allows us to determine the inhibition percentage of the fungal growth, by measuring colony diameters on agar plates and assessing the effect of the medium composition where they are growing. In order to set the concentration of experimental additives to test in culture media, the amount of silver and copper in each solid was taking into account. At the same time, plates were prepared, as controls, adding the same amount of the solids to be test, without Ag in their composition. Petri dishes were prepared with 15 mL of the culture media (CM agar): 2.5 g glucose, 1.25 g peptone, 0.25 g KH_2PO_4, 0.125 g $MgSO_4$ $7H_2O$, 4.0 g of agar and up to 250 mL of distilled water.

Then, 0.001, 0.01 or 0.05% (weight/volume) of Ag or Cu was added to the medium, in relation to the content of metal of the tested solids and, on the other hand, the equivalent solids, without Ag or Cu in their composition, were added in the same amount to CM-agar plates. Finally, controls without any additive were prepared. Triplicates were set up for each concentration, including the controls. The petri dishes were inoculated in the center

with 20 μL of spores suspension (10^5 spores/mL) of *Alternaria alternata* or *Chaetomium globosum*, and then incubated at 28 ± 1 °C for 9 and 10 days, with the respective fungus. With the obtained results, the inhibition percentage (I %) was calculated according to the following equation (1):

$$Inhibition\ (\%) = [(C-E)/C] \times 100$$

where C and E correspond to the average diameter of each fungus in the control plate and on the plate with the tested solids, respectively. Three measurements of the fungal growth diameter were made in each plate and standard deviation was determined.

3. Results and Discussion

3.1. Characterization of the solids

Table 1 shows the textural properties (S_{BET}, pore volume and pore size) and % moisture, zeta potential and acidity (E_i) values of the synthesized solids. Regarding the textural properties, as it can be observed in Table 1, the samples presented high S_{BET} values, being the sample with the highest superficial area the unmodified silica (741.3 m^2/g). The ashes showed a very low value of S_{BET} (5 m^2/g, almost coincident with the error of the technique) therefore, when different amounts of ashes were incorporated in the synthesis the area of the silica decreased to 643.3 m^2/g for 1% ashes and to 284.9 m^2/g for 10% ashes. A similar behavior was observed in Ag-silica and Cu-silica with different amounts of ashes; and samples containing 1 % of ashes maintain a surface area value similar to the unmodified silica, while with 10% of ashes the surface area decreases.

The N_2 adsorption-desorption curves obtained for the synthesized solids are showed in Figure 2. These curves indicate that the variation in the pore size and the surface area are consistent with the results of the curve hysteresis, showing Type IV isotherms, with hysteresis loop H_2, according to the classification given by Brunauer et al., characterized by a wide hysteresis loop and a pronounced plateau [41; 42], characteristics of highly mesoporous materials while H_2 loop is normally observed for ink bottled shaped pores [43].

Table 1 Textural properties: S_{BET}, pore volume and pore size of the solids synthesized

	S_{BET} (m^2/g)	Pore Volume (cm^3/g)	Pore Size (Å)	% Moisture	Zeta Potential (mV)	E_i (mV)
S0	741.3	0.78	42.3	6.59 ± 0.28	-22.5 ± 4.38	104
SA-1	643.3	0.55	34.2	6.64 ± 0.75	-20.8 ± 4.94	104
SA-10	284.9	0.33	47.3	9.33 ± 0.52	-20.1 ± 5.04	266
SAAg-1-1	672.6	0.76	45.4	5.24 ± 0.79	-20.3 ± 4.20	82
SAAg-1-2	654.7	0.62	37.8	7.35 ± 1.17	-22.0 ± 5.20	100
SAAg-10-1	335.9	0.43	51.5	6.93 ± 0.57	-20.1 ± 4.64	207
SAAg-10-2	318.8	0.50	63.1	8.95 ± 0.27	-22.6 ± 4.10	196
SACu-1-1	501.5	0.54	42.9	8.29 ± 0.81	-18.3 ± 4.79	124
SACu-1-2	640.0	0.69	43.0	7.42 ± 0.30	-18.1 ± 3.46	96
SACu-10-1	406.9	0.48	47.1	7.37 ± 0.53	-20.5 ± 5.42	261
SACu-10-2	399.7	0.42	42.3	6.76 ± 0.60	-18.4 ± 5.34	205
Ashes	5	0.01	93.2	6.21 ± 1.16	-24.7 ± 6.38	-20

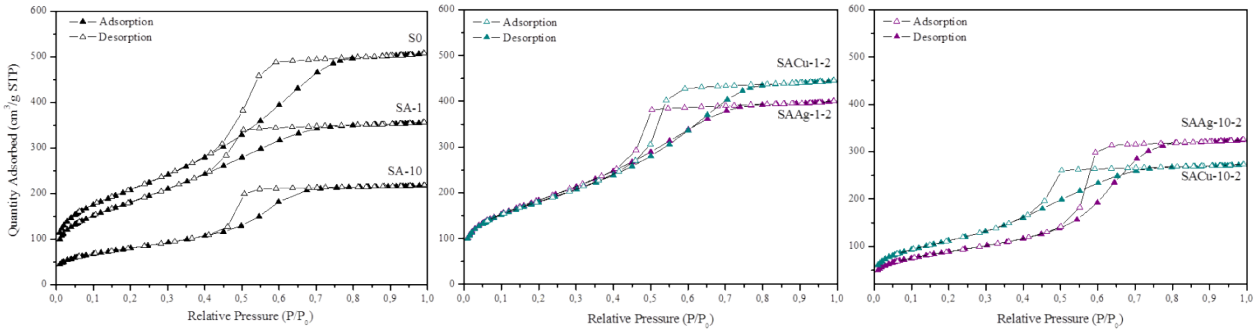

Figure 2 Adsorption-desorption isotherms of S0, SA-1 and SA-10 samples

In relation to the moisture content, it was less than 10% in all the samples synthesized and no variation was observed with the addition of sunflower ashes.

Zeta potential is a relevant parameter to understand the state of the particle surface and for seeing its long-term stability. The higher the zeta potential, the stronger the repulsion and the more stable the system becomes [42]. Particles with a zeta potential between -10 and +10 mV are considered approximately neutral, while nanoparticles with zeta potentials greater than +30 mV or less than -30 mV are considered strongly cationic and strongly

anionic, respectively. In all the synthesized samples, stable particles negatively charged were observed.

The electrode potential difference (E) was employed to determine the acid properties of the solids by the potentiometric titration with *n*-butylamine. Initial electrode potential values (E_i) indicate the maximum acidic force of superficial sites and this acid strength can be classified according to the following ranges: very strong sites, $E_i > 100$ mV, strong sites, $0 < E_i < 100$ mV; weak sites $-100 < E_i < 0$ mV, and very weak sites, $E_i < -100$ mV [44; 45]. As shows Table 1, unmodified silica (S0) present strong acid sites (104 mV) in contrast with the sunflower ashes that show weak sites (-20 mV). No changes in potential electrode values was observed with the addition of ashes at a concentration of 1% wt. in the synthesis of the solids, but when ashes were added at a concentration of 10% wt. the maximum acidic force of superficial sites was duplicated. In general, when silver or copper was incorporated into the synthesis, a decrease of the E_i values was observed, mainly when the concentration of ashes was of 10% wt. This decrease could be due to the common ion effect, and the addition of nitrate ions from the salts would produce the suppression of the degree of dissociation of the weak electrolyte from the nitric acid. However, the acidity obtained in all the samples should be appropriate to be used as fillers in antimicrobial materials [40; 46].

The FT-IR spectra of the ashes, the unmodified S0, SA-1 and SA-10 samples are shown in Figure 3 and FT-IR spectra of samples with silver and copper and 1 and 10% w/w of ashes are shown in Figure 4. The spectra of the synthesized samples showed the characteristic bands of SiO_2. Around 3400 cm^{-1}, a wide band assigned to stretching vibrations of water molecules bonding to superficial silanol groups (OH and SiO-H) [47; 48] is observed, at 1640 cm^{-1} appears a band associated with the adsorption of water in the surface and is assigned to the angular deformation of molecular water (H-O-H) and finally, at 950 cm^{-1} is assigned to the vibration of Si-OH bonds [49]. Those absorption bands indicate the presence of hydrophilic silica xerogel, with high amount of molecular water and hydroxyls groups. Also, well defined bands were observed at 1200 cm^{-1}, 1080 cm^{-1} and 800 cm^{-1}. The first two bands are assigned to asymmetric stretching modes (Si-O) and the last one is associated to the symmetric stretching mode (Si-O-Si) or vibrational modes of ring structures. At lower wavenumbers, the band at 460 cm^{-1} corresponds to the bending

vibration mode of the SiO_4 tetrahedron or symmetric oxygen stretching vibrations of surface silanol and finally, the band around 560 cm^{-1} is attributed to four-member siloxane rings deformation, stables during de hydrolysis process, so them can constitute a great fraction of the olygomeric species in TEOS systems [49].

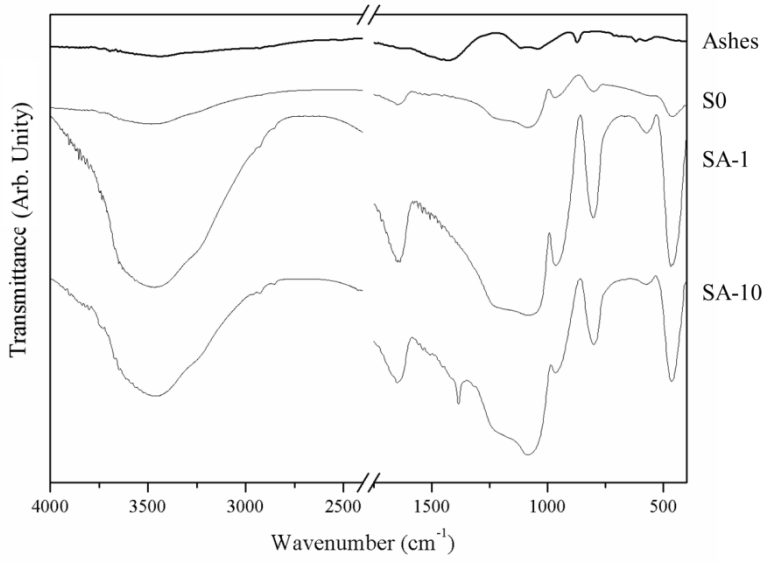

Figure 3 FT-IR spectra of ashes, S0, SA-1 and SA-10 samples

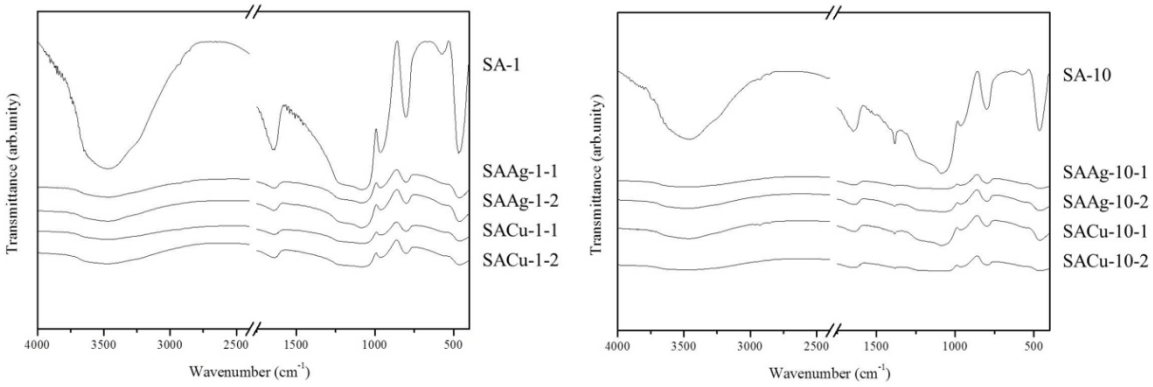

Figure 4 FT-IR spectra of samples with silver and copper and 1 and 10% w/w of ashes

Changes in shape and position of the peaks in the absorption bands may be associated to structural changes, produced by different compositions of water or reagents, and leading to a variation in hydrolysis and condensation ratios. The bands of the modified solids with the silver and copper salts showed no significant differences in form, spectra not shown. Neither difference was found between the spectra of solids modified with different amounts

of ashes.

On the other hand, the SEM micrographs of the ashes sample, the unmodified silica and the samples with 1 and 10% wt. of ashes, at different magnifications, are displayed in Figure 5. Regarding to the modified samples, with different amounts of salts or ashes, they are similar in morphology to the unmodified silica (S0), maintaining the characteristic laminar morphology of amorphous silica. Also, all the particles formed are irregular in shape and structure. In relation to the SEM-EDS and elemental analysis of the samples with Ag or Cu (Figure 6), a homogeneous distribution of the components in the silica matrix was observed, with few less-concentrated areas.

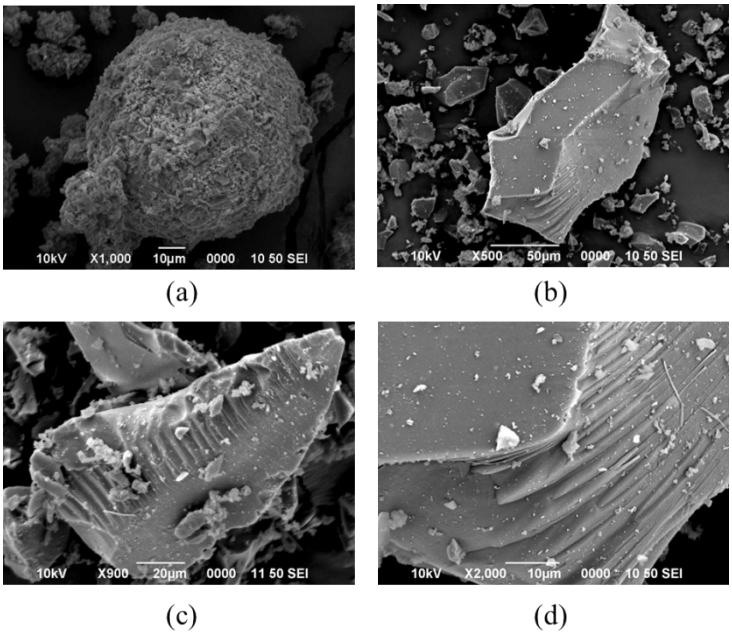

Figure 5 SEM micrographs of (a) ashes, (b) S0, (c) SA-1 and (d) SA-10 samples

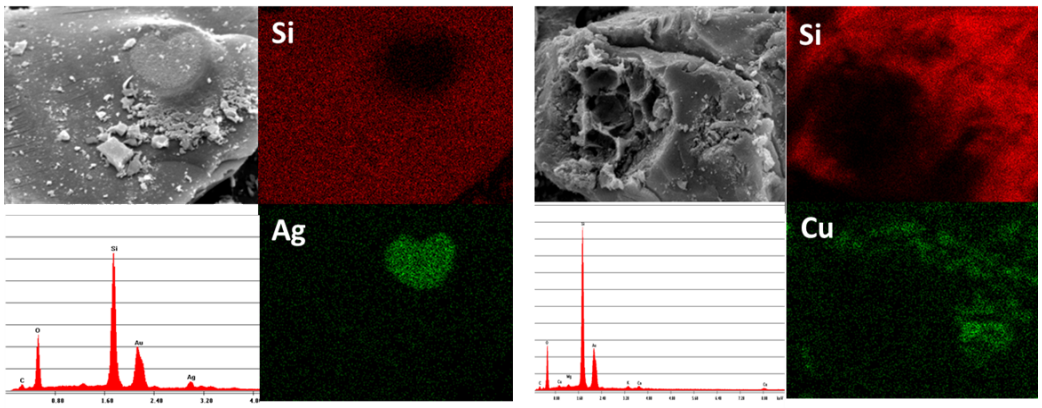

Figure 6 SEM micrographs and mapping of (a) SAAg-10-2 and (b) SACu-10-2 samples

The TEM images of unmodified silica and SA-10 sample (Figure 7a and 7b) show that the Si framework consists of interconnected small primary particles result of the acid synthesis. In addition to this, in silver-silica (Figure 7c and 7d) and copper-silica (Figure 7e and 7f) nanoparticles can be clearly seen embedded in the oxide matrix being essentially spherical in shape. In Ag-silica samples with 1% of ashes, SAAg-1-1 (Figure 7c) and SAAg-1-2, spherical particles with size between 10 and 100 nm and dendritic particles like flowers are observed. It has been shown that the morphology of crystals depends on the distance of the formation conditions from thermodynamic equilibrium, been the spherical particles close to equilibrium and dendritic nanostructures away from it [50]. When ashes were added in an amount of 10%, SAAg-10-1 (Figure 7d) and SAAg-10-2 samples, only spherical Ag-nanoparticles were present with small size, around 10 nm. Regarding the synthesis of silica with a cupric salt, in samples with 1% of ashes, SACu-1-1 (Figure 7e) and SACu-1-2, copper nanoparticles supported on silica were obtained and the average nanoparticle size was 10 nm, whereas with 10% of ashes, SACu-10-1 (Figure 7f) and SACu-10-2 the formation of nanoparticles (NPs) were not observed.

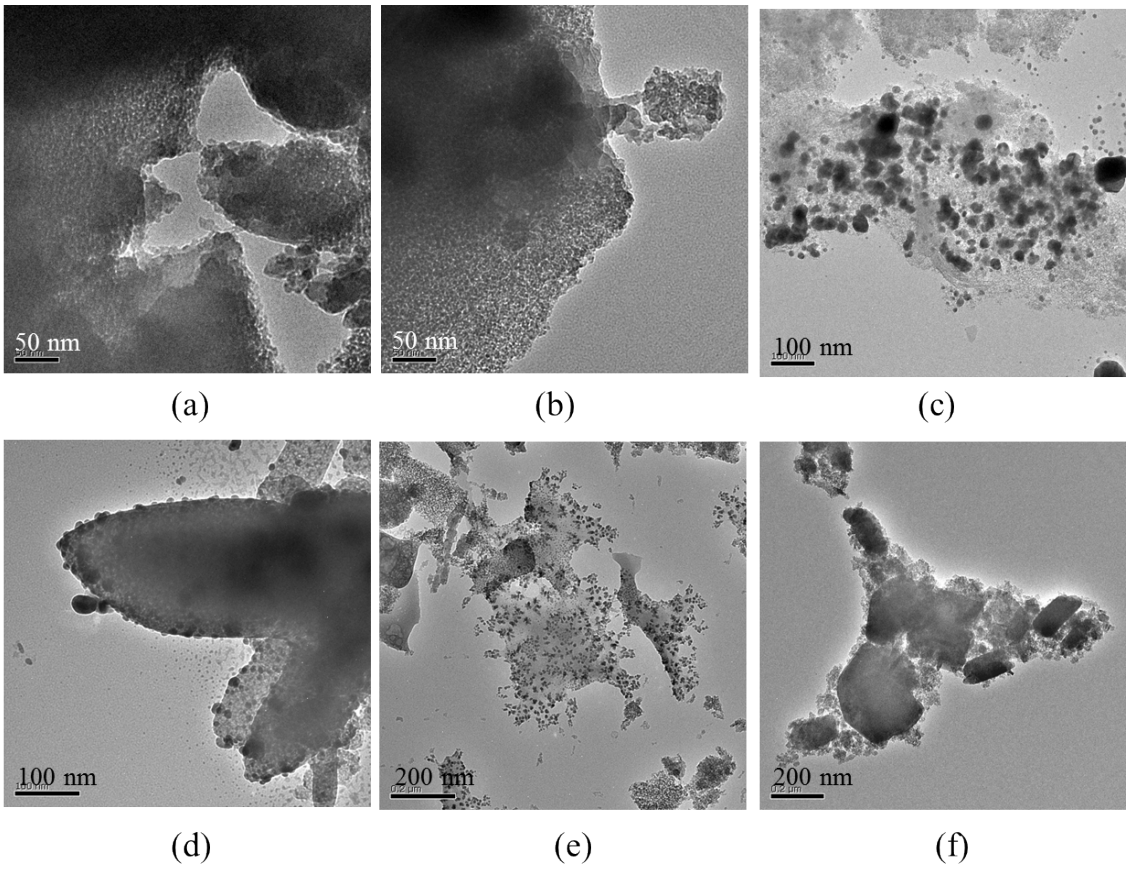

Figure 7 TEM micrographs of (a) unmodified silica S0 (bar: 50 nm), (b) SA-10 (bar: 50 nm), (c) SAAg-1-1 (bar: 100 nm), (d) SAAg-10-1 (bar: 100 nm), (e) SACu-1-1 (bar: 200 nm) and (f) SACu-10-1 (bar: 200 nm)

According to Adegboyega et al. [51], metal salts in the presence of organic acids could help the formation of silver nanoparticles due to the reduction of ions (Ag^{+} or Cu^{+2}) by the functional groups found in the organic matter, specifically the presence of free radicals and carboxylic or phenolic groups. But, when the amount of ashes was greater (10% w/w), the negatively charged groups could prevent agglomeration of NPs by electrostatic repulsion and provide a better stability of the colloidal suspension, being the nanoparticles formed smaller and even ionic silver and ionic copper would be present in majority amount in these samples.

3.2. Antifungal activity

The antifungal activity of the additives was assessed, employing an in vitro fungal growth inhibition assay, by measuring the colony diameters on CM-agar over time. Figure 8 shows selected photographic registers of the antifungal assay with selected silica, against *C. globosum* and *A. alternata* and Table 2 presents the inhibition percentages (%I) calculated employing Eq. (1), for all the concentrations used.

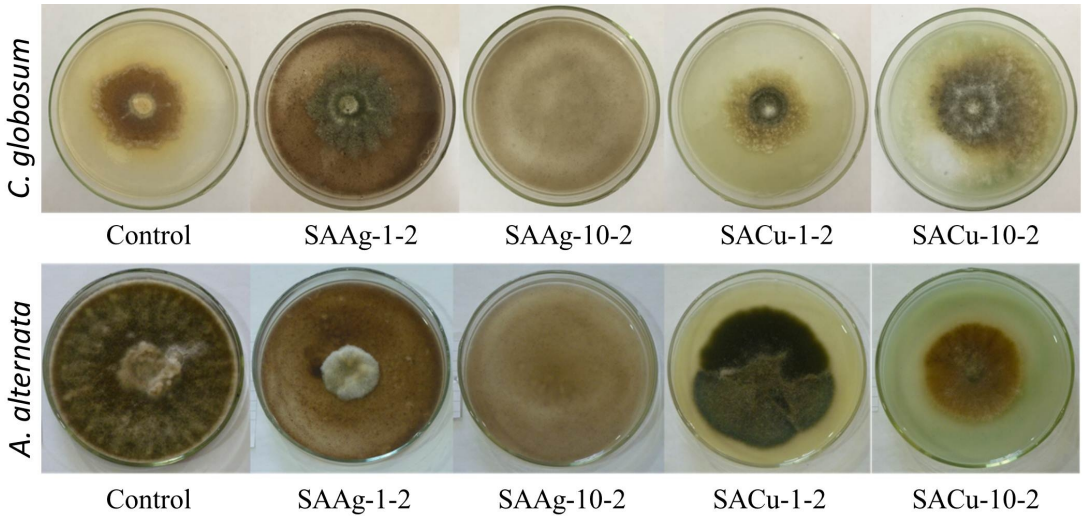

Figure 8 Fungal growth in CM-agar plates, after a week at 28 ± 1 °C with and without 0.05% (w/v) of the additives

Table 2 Inhibition percentages calculated at different additive concentrations

	C. globosum			***A. alternata***		
	0.001% w/v	**0.01% w/v**	**0.05% w/v**	**0.001% w/v**	**0.01% w/v**	**0.05% w/v**
SA-1	NI	NI	NI	1.8	2.5	3.1
SA-10	NI	NI	3.3	2.4	3.5	3.6
SAAg-1-2	NI	NI	8.8	2.8	63.0	80.0
SAAg-10-2	10.1	97.4	100	51.8	92.9	100
SACu-1-2	NI	NI	1.9	1.6	10.1	21.1
SACu-10-2	NI	NI	NI	1.3	3.1	41.7

Without the presence of silver or copper, neither the solids with 1% of ashes nor the solids with 10% of ashes showed antifungal activity. We found that the solids synthesized with Ag or Cu inhibited the fungal growth and *A. alternata* fungus was more sensitive than *C. globosum* at the concentrations used. It should be noted that the addition of a higher amount of ashes increased the antifungal activity of the solids, especially in Ag-silica. The solids with an intermediate concentration of Ag (0.01%) and 10% of ashes showed a growth inhibition higher than 90% against both fungi. In the case of *C. globosum*, from not being inhibited (NI) in sample with 1% of ashes, by the adding 10% of ashes, the inhibition increases up to 97% and, when the silver concentration was 0.05%, no growth was observed with both fungi. Even with a concentration as low as 0.001% of silver the silica with 10% of ashes was able to inhibit the 50% of *A. alternata* growth. This fungus is a real threat to human health and is often found inside houses deteriorating the environmental quality for its occupants. A possibly approach to explain these results is taking account properties exhibited for the silica synthesized. According to the characterization, an increase in the amount of ashes in solids led to obtain smaller metal nanoparticles in Ag-samples and a greater amount of silver and copper ions into the matrix. These two factors could be affecting positively the antimicrobial activity of the solids, which is believed is based on the combination of the action of both, ions and particles [52]. Also, humidity is a key factor for ion transportation and also a trigger for silver ions generation which process would be favored by acidic environment [53]. Therefore, the conditions created in the solids synthesized with 10% of ashes seem to be more favorable for the antimicrobial action. Copper silica did not show such high inhibition values as silver silica at the concentrations tested, probably due to the fact that copper ions are less effective than silver ions, and higher concentrations need to be used to obtain the same antimicrobial activity.

4. Conclusions

It was possible to obtain mesoporous solids, by the sol-gel method at room temperature, with silver and copper ions and nanoparticles, to be used as bioactive material with antifungal activity. The addition of ashes into the solids improved the antifungal activity of the silica due to a greater amount of ionic silver and ionic copper would be

present in these samples. These results are very promising since the ash is a waste product without commercial value that proved to be useful in the development of new bioactive materials to prevent fungal infections.

The use of Ag or Cu fillers results in a controlled spread of microorganisms in internal environments that could improve the quality of life and human health with the use of green chemistry principles.

Acknowledgements

The authors would like to express their thanks for the financial support provided by National Scientific and Technical Research Council (CONICET) and National University of La Plata (UNLP). To Graciela Valle for FT-IR spectra, Lilian Osiglio for potenciometric tritration and Edgardo Soto for textural properties measurements. They also thank to Melisa Palma for providing SEM images, Reynaldo Pereira for TEM micrographs from LANOTEC.

References

[1] B.J. Brown, M.E. Hanson, D.M. Liverman, R.W. Merideth Jr., Global sustain-ability: Toward definition, Environ. Manag. 11 (1987) 713-719.

[2] G.H. Brundtland, Our common future: report of the world commission on environment and development, Med. Confl. Surviv. 4 (1987) 300.

[3] N. Wise, Outlining triple bottom line contexts in urban tourism regeneration, Cities 53 (2016) 30-34.

[4] L. Acero, P. Savaget, Plural understandings of sociotechnical progress within the OECD. In: 12th Globelics International Conference, 19e31 October 2014 (Addis Ababa, Ethiopia).

[5] M. Geissdoerfer, P. Savaget, N. Bocken, E.J. Hultink, The Circular Economy e A new sustainability paradigm?, J. Cleaner Production 143 (2017) 757-768.

[6] I.N. Soyiri, D.D. Reidpath, An overview of health forecasting, Environ Health Prev Med. 18 (2013) 1-9.

[7] A. Chang, E.M. Lad, S.P. Lad, Hippocrates' influence on the origins of neurosurgery. Neurosurg Focus 23 (2007) E9.

[8] J.C.A. Janssens, H. Steenackers, S. Robijns, E. Gellens, J. Levin, H. Zhao, K. Hermans, D. De Coster, T.L. Verhoeven, K. Marchal, J. Vanderleyden, D.E. De Vos, S.C.J. De Keersmaecker, Appl. Environ. Microbiol. 74 (2008) 6639.
[9] A. Kramer, I. Schwebke, G. Kampf, How long do nosocomial pathogens persist on inanimate surfaces? A systematic review, BMC Infect. Dis. (2006).
[10] F. Siedenbiedel, J.C. Tiller, Antimicrobial Polymers in Solution and on Surfaces: Overview and Functional Principles, Polymers 4 (2012) 46.
[11] M.A. Fernández, N. Bellotti, Silica-based bioactive solids obtained from modified diatomaceous earth to be used as antimicrobial filler material, Mater. Lett. 194 (2017) 130-134.
[12] R. Lu, W. Zou, H: Du, J. Wang, S. Zhang, Antimicrobial activity of Ag nanoclusters encapsulated in porous silica nanospheres, Ceram Int, 40 (2014) 3693–3698.
[13] H. Kong, J. Jang, Antibacterial properties of novel poly(methyl methacrylate) nanofiber containing silver nanoparticles, Langmuir 24 (2008) 2051.
[14] R. Ciriminna, A. Fidalgo, V. Pandarus, F. Béland, L.M. Ilharco, M. Pagliaro, The sol-gel route to advanced silica-based materials and recent applications, Chem. Rev. 113 (2013) 6592.
[15] G.J. Copello, S. Teves, J. Degrossi, M. D'Aquino, M.F. Desimone, L.E. Diaz, Antimicrobial activity on glass materials subject to disinfectant xerogel coating, J. Ind. Microbiol. Biotechnol. 33 (2006) 343.
[16] M. Marini, M. Bondi, R. Iseppi, M. Toselli, F. Pilati, Preparation and antibacterial activity of hybrid materials containing quaternary ammonium salts via sol–gel process, Eur. Polym. J. 43 (2007) 3621.
[17] S.A.H. Jalali, A.R. Allafchian, S.S. Banifatemi, I. Ashrafi Tamai, The antibacterial properties of Ag/TiO2 nanoparticles embedded in silane sol–gel matrix, J. Taiwan Inst. Chem. Eng. 66 (2016) 357-362.
[18] B. Samuneva, Y. Dimitriev, V. Dimitrov, E. Kashchieva, G. Encheva, Silica Gels and Gel Glasses Containing Silver and Platinum Metal Particles, J. Sol-Gel Sci. Technol. 13 (1998) 969-974.
[19] G. Gosheger, J. Hardes, H. Ahrens, A. Streitburger, H. Buerger, M. Erren, A. Gunsel,

F.H. Kemper, W. Winkelmann, C. Von Eiff, Silver-coated megaendoprostheses in a rabbit model--an analysis of the infection rate and toxicological side effects, Biomaterials 25 (2004) 5547-5556.
[20] M.E. Rupp, T. Fitzgerald, N. Marion, V. Helget, S. Puumala, J.R. Anderson, P.D. Fey, Effect of silver-coated urinary catheters: efficacy, cost-effectiveness, and antimicrobial resistance, Am. J. Infect. Control. 32 (2004) 445-450.
[21] N. Bellotti, R. Romagnoli, C. Quintero, C. Domínguez-Wong, F. Ruiz, C. Deyá, Nanoparticles as antifungal additives for indoor water borne paints, Prog. Org. Coat. 86 (2015) 33-40.
[22] H.J. Lee, S.Y. Yeo, S.H. Jeong, Antibacterial effect of nanosized silver colloidal solution on textile fabrics, J. Mater. Sci. 38 (2003) 2199-2204.
[23] M. Zielecka, E. Bujnowska, B. Kępska, M. Wenda, M. Piotrowska, Antimicrobial additives for architectural paints and impregnates, Prog. Org. Coat. 72 (2011) 193-201.
[24] J. Natsuki, T. Natsuki, Y. Hashimoto, A Review of Silver Nanoparticles: Synthesis Methods, Properties and Applications, Int. J. Mater. Sci. Appl. 4 (2015) 325-332.
[25] T.V. Duncan, Applications of nanotechnology in food packaging and food safety: barrier materials, antimicrobials and sensors, J. Colloid Interface Sci. 363 (2011) 1-24.
[26] R.E. Morsi, A.M. Alsabagh, S.A. Nasr, M.M. Zaki, Multifunctional nanocomposites of chitosan, silver nanoparticles, copper nanoparticles and carbon nanotubes for water treatment: Antimicrobial characteristics, Int. J. Biol. Macromol. 97 (2017) 264-269.
[27] C. Fan, L. Chu, H.R. Rawls, B.K. Norling, H.L. Cardenas, K. Whang, Development of an antimicrobial resin-a pilot study, Dent. Mater. 27 (2011) 322-328.
[28] L. Windler, M. Height, B. Nowack, Comparative evaluation of antimicrobials for textile applications, Environ. Int. 53 (2013) 62-73.
[29] R. Arreche, N. Bellotti, M: Blanco, P. Vázquez, Improved antimicrobial activity of silica–Cu using a heteropolyacid and different precursors by sol–gel: synthesis and characterization, J. Sol-Gel Sci. Technol. 75 (2015) 374-382.
[30] H. Palza, K. Delgado, N. Curotto, Synthesis of copper nanostructures on silica-based particles for antimicrobial organic coatings, Appl. Surf. Sci. 357 (2015) 86-90.
[31] J.P. Ruparelia, A.K. Chatterjee, S.P. Duttagupta, S: Mukherji, Strain specificity in

antimicrobial activity of silver and copper nanoparticles, Acta Biomater. 4 (2008) 707-716.
[32] J. Andas, F. Adam, One-pot synthesis of nanoscale silver supported biomass-derived silica, Mater. Today: Proc. 3 (2016) 1345.
[33] H.J. Jeon, S.C. Yi, S.G. Oh, Preparation and antibacterial effects of Ag-SiO_2 thin films by sol-gel method, Biomaterials 24 (2003) 4921-4928.
[34] N. Quaranta, M. Unsen, H. López, C. Giansiracusa, J.A. Roether, A.R. Boccaccini, Ash from sunflower husk as raw material for ceramic products, Ceram. Int. 37 (2011) 377.
[35] Food and Agriculture Organization of the United Nations (FAO). Agriculture Data. Available online: http://www.fao.org/faostat/en/#home (accessed on 13 May 2018).
[36] G. Zajac, J. Szyszlak-Bargłowicz, M. Szczepanik, Influence of Biomass Incineration Temperature on the Content of Selected Heavy Metals in the Ash Used for Fertilizing Purposes. Appl. Sci. 9 (2019) 1790.
[37] M.A. Perea-Moreno, F. Manzano-Agugliaro, A.J. Perea-Moreno, Sustainable Energy Based on Sunflower Seed Husk Boiler for Residential Buildings, Sustainability 10 (2018) 3407.
[38] G. Maj, P. Krzaczek, A. Kuranc, W. Piekarski, Energy Properties of Sunflower Seed Husk as Industrial Extrusion Residue, Agricultural Engineering 21 (2017) 77-84.
[39] O.C.G. Adan, R.A. Samson, 2011. Fundamentals of mold growth in indoor environments and strategies for healthy living, Wageningen Academic Publishers.
[40] R. Arreche, K. Igal, N. Bellotti, Síntesis verde y caracterización de sólidos de matriz silícea con cobre y plata obtenidos a partir de dos precursores para su aplicación como aditivos antifúngicos, Revista Materia 20 (2015) 612–620.
[41] E.T.S. Brunauer, P.H. Emmett, Adsorption of Gases in Multimolecular Layers, J. Am. Chem. Soc. 60 (1938) 309-319.
[42] Gregg, S. J.; Sing, K. S. W.; Adsorption, Surface Area and Porosity, Acad. Press, 1982
[43] F. Adam, J. Andas, I.A. Rahman, A study on the oxidation of phenol by heterogeneous iron silica catalyst, Chem. Eng. J. 165 (2010) 658-667.
[44] P. Villabrille, P. Vázquez, M. Blanco, C. Cáceres, Equilibrium Adsorption of Molybdosilicic Acid Solutions on Carbon and Silica: Basic Studies for the Preparation of Ecofriendly Acidic Catalysts, J. Colloid Interface Sci. 251 (2002) 151-159.

[45] L.R. Pizzio, P.G. Vázquez, C.V. Cáceres, M.N. Blanco, Supported Keggin type heteropolycompounds for ecofriendly reactions, Appl. Catal. A 256 (2003) 125-139.
[46] R. Arreche, N. Bellotti, C. Deyá, P. Vázquez, Assessment of waterborne coatings formulated with sol-gel/Ag related to fungal growth resistance, Prog. Org. Coat. 108 (2017) 36-43.
[47] A. Duran, C. Serna, V. Fornes, J.M. Fernandez Navarro, Structural considerations about SiO_2 glasses prepared by sol-gel, J. Non-Cryst. Solids 82 (1986) 69-77.
[48] G. Orcel, J. Phalippou, L.L. Hench, Structural changes of silica xerogels during low temperature dehydration, J. Non-Cryst. Solids 88 (1986) 114-130.
[49] C. Araujo-Andrade, G. Ortega-Zarzosa, S. Ponce-Castañeda, J.R. Martínez, F. Villegas-Aguirre, F: Ruiz, Rev. Mex. Fis. 46 (2000) 593.
[50] X.K. Meng, S.C. Tang, S. Vongehr, A Review on Diverse Silver Nanostructures, J. Mater. Sci. Technol. 26 (2010) 487-522.
[51] N.F. Adegboyega, V.K. Sharma, K. Siskova, R. Zboril, M. Sohn, B.J. Schultz, S. Banerjeet, Interactions of Aqueous Ag^+ with Fulvic Acids: Mechanisms of Silver Nanoparticle Formation and Investigation of Stability, Environ. Sci. Technol. 47 (2013) 757-764.
[52] C. Dominguez-Wong, G.M. Loredo-Becerra, C.C. Quintero-González, M.E. Noriega-Treviño, M.E. Compeán-Jasso, N. Niño-Martínez, I. Dealba-Montero, F. Ruiz, Evaluation of the antibacterial activity of an indoor waterborne architectural coating containing Ag/TiO_2 under different relative humidity environments, Mater. Lett. 134 (2014) 103-106.
[53] Z. Xiu, Q. Zhang, H.L. Puppala, V.L. Colvin, P.J.J. Alvarez, Negligible particle-specific antibacterial activity of silver nanoparticles, Nano Lett. 12 (2012) 4271-4275.

Figures captions